Synthesis, biological evaluation and molecular modeling studies of imidazo[1,2- a]pyridines derivatives as protein kinase inhibitors

Marie Lawson, Jordi Rodrigo, Blandine Baratte, Thomas Robert, Claire Delehouzé, Olivier Lozach, Sandrine Ruchaud, Stéphane Bach, Jean-Daniel Brion, Mouad Alami, et al.

European Journal of Medicinal Chemistry 123 (2016) 105–114

Contents lists available at ScienceDirect

European Journal of Medicinal Chemistry

journal homepage: http://www.elsevier.com/locate/ejmech

Research paper

Synthesis, biological evaluation and molecular modeling studies of imidazo[1,2-*a*]pyridines derivatives as protein kinase inhibitors

Marie Lawson [a], Jordi Rodrigo [a], Blandine Baratte [b], Thomas Robert [b], Claire Delehouzé [b], Olivier Lozach [b], Sandrine Ruchaud [b], Stéphane Bach [b], Jean-Daniel Brion [a], Mouad Alami [a, **], Abdallah Hamze [a, *]

[a] *BioCIS, Univ. Paris-Sud, CNRS, équipe labellisée Ligue Contre le Cancer, Université Paris-Saclay, 92290, Châtenay-Malabry, France*
[b] *Sorbonne Universités, UPMC Univ Paris 06, CNRS USR3151, "Protein Phosphorylation and Human Disease" Unit, Plateforme de criblage KISSf, Station Biologique de Roscoff, Place Georges Teissier, 29688, Roscoff, France*

ARTICLE INFO

Article history:
Received 18 May 2016
Received in revised form
23 June 2016
Accepted 19 July 2016
Available online 21 July 2016

Keywords:
CLK1
DYRK1A
Kinase inhibitors
Imidazo[1,2-*a*]pyridines

ABSTRACT

We report here the synthesis, the biological evaluation and the molecular modeling studies of new imidazo[1,2-*a*]pyridines derivatives designed as potent kinase inhibitors. This collection was obtained from 2-aminopyridines and 2-bromoacetophenone which afforded final compound in only one step. The bioactivity of this family of new compounds was tested using protein kinase and ATP competition assays. The structure-activity relationship (SAR) revealed that six compounds inhibit DYRK1A and CLK1 at a micromolar range. Docking studies provided possible explanations that correlate with the SAR data. The most active compound **4c** inhibits CLK1 (IC_{50} of 0.7 μM) and DYRK1A (IC_{50} of 2.6 μM).

1. Introduction

Protein kinases are a ubiquitous group of enzymes sharing structural similarities and are involved in various biological processes within the cell [1,2]. They catalyze the transfer of phosphoryl group from a phosphate donor (usually ATP) to a receptor substrate, which can be a small molecule, lipid, or protein substrate. Kinase deregulation is frequently observed during the development of human diseases such as cancer [3], neurodegenerative disease including Alzheimer's disease (AD) [4,5], inflammation or diabetes [6]. Protein kinases are attractive targets for structure-based drug discovery projects because of their crucial role in physiological pathways. Over the past decades, protein kinases become attractive targets for structure-based drug discovery projects and are a substantial and growing part of most major pharmaceutical companies' drug target portfolios [2,7–9].

Nature is a source of new chemical scaffolds which could be an excellent basis for rational structure-based design. In this context, harmine is β-carboline compound that is naturally found in several medicinal plants including *Peganum harmala* (Zygophyllaceae) and *Banisteriopsis caapi* (Malpighiaceae) [10,11]. Leucettine L41 [12] a synthetic analogue of Leucettamine B, a compound extracted from the sponge *Leucetta microporis* in 1993 [13], inhibit various kinases and especially CLK1 (CDC2-like Kinase 1) and DYRK1A (dual-specificity tyrosine phosphorylation-regulated kinase1A) at a submicromolar range. Synthesis of a range of analogues of harmine and leucettine L41, including **1** [14] and **2** [15] was undertaken to understand and study biological activities of these molecules (Fig. 1). Compounds **1** and **2** have a moderate inhibitory activity on CLK1 and DYRK1A are less potent inhibitors of these kinases than reference compounds. Furthermore, a new series of compounds of type imidazo[1,2-*a*]pyridine **3** [16], has nanomolar activity against CDK-(Cyclin-Dependent Kinase) 1 and 2, leading to compound **3** blocking the cell cycle and hence 3 could have utility in cancer treatment.

High-throughput screening (HTS) has become increasingly important for hit identification in drug discovery [17]. The increasing number of compounds available for screening and recent advances in robotic are the driving forces for the development of elaborated assay systems. This new technology led scientists to discover new active compounds. High-throughput kinase-based screening of small molecules is an attractive strategy to

* Corresponding author.
** Corresponding author.
E-mail address: abdallah.hamze@u-psud.fr (A. Hamze).

http://dx.doi.org/10.1016/j.ejmech.2016.07.040
0223-5234/

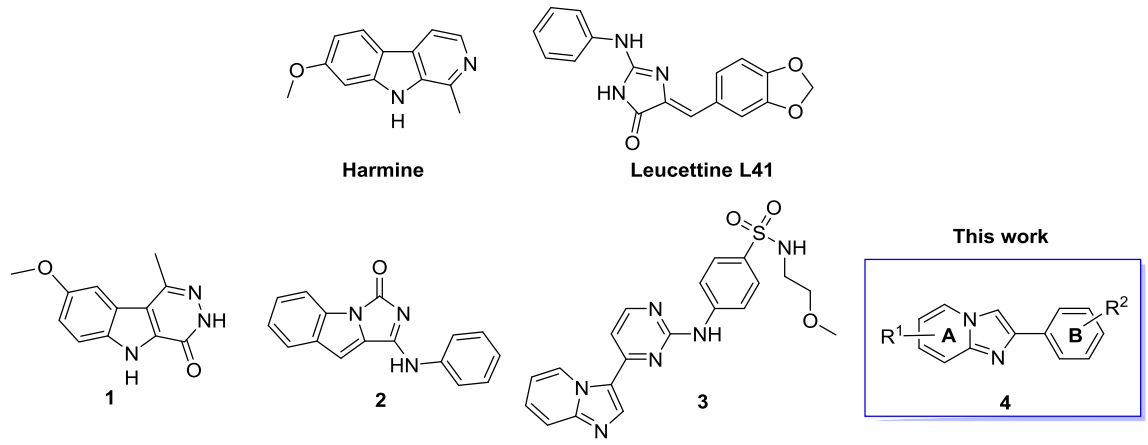

Fig. 1. Structures of Harmine, its analogues **1**, Leucettine L41, its analogue **2** and imidazo[1,2-*a*]pyridines **3** and our new structures **4**.

Table 1
Synthesis of imidazo[1,2-*a*]pyridines **4a-4j** by changing the nature of ring **A**.

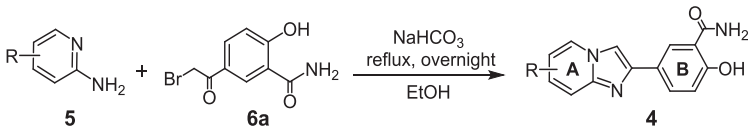

Entry	2-Aminopyridine 5		Imidazo[1,2-*a*]pyridine 4		Yields (%)[a]
1	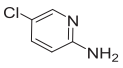	**5a**	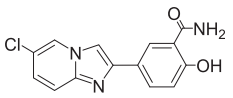	**4a**	65
2	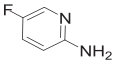	**5b**	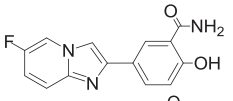	**4b**	35
3	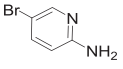	**5c**	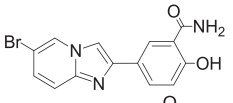	**4c**	40
4	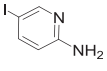	**5d**	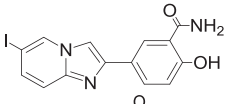	**4d**	30
5		**5e**	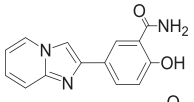	**4e**	75
6	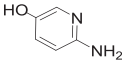	**5f**	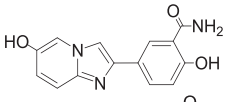	**4f**	16
7	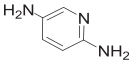	**5g**	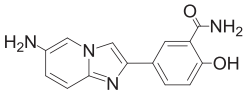	**4g**	8
8	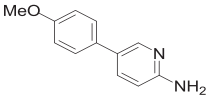	**5h**	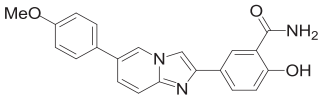	**4h**	50
9	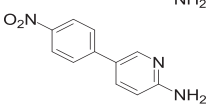	**5i**	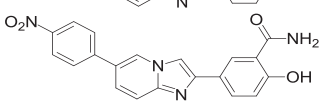	**4i**	25
10		**5j**	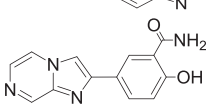	**4j**	12

[a] Isolated yields. General conditions: 2-bromoacetophenone **6** (1.05 mmol), 2-aminopyridine **5** (1.0 mmol) and $NaHCO_3$ (2.0 mmol) in EtOH (20 mL), reflux, overnight.

Table 2
Synthesis of imidazo[1,2-*a*]pyridines **4k-4r** by changing the nature of ring **B**.

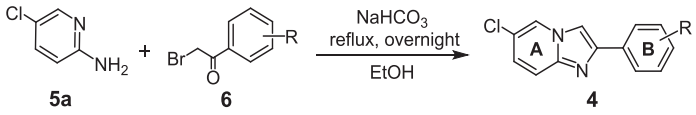

5a 6 4

Entry	2-Bromoacetophenone 6		Imidazo[1,2-*a*]pyridine 4		Yields (%)[a]
1	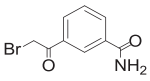	**6b**	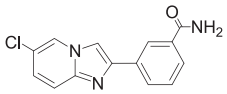	**4k**	20
2	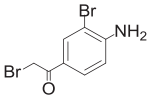	**6c**	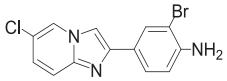	**4l**	40
3	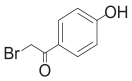	**6d**	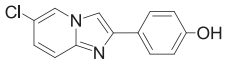	**4m**	22
4	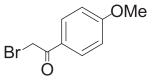	**6e**	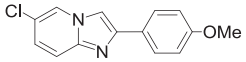	**4n**	10
5	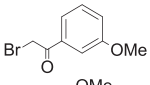	**6f**	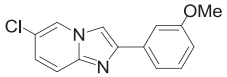	**4o**	62
6	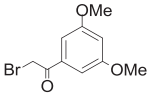	**6g**	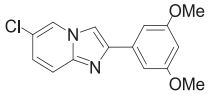	**4p**	46
7	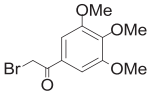	**6h**	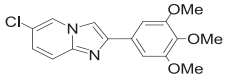	**4q**	40
8	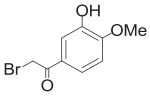	**6i**	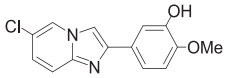	**4r**	38

[a] Isolated yield.

identify such agents. We screened a library of 110 compounds of our synthesized in-house collection against a panel of kinases. A distinct kinase selectivity profile was observed for the molecule containing the imidazo[1,2-*a*]pyridines scaffold. Therefore, compound **4a** (Table 1) was identified as a selective kinase inhibitor with micromolar activity against CLK1 (CDC2-like Kinase 1) and DYRK1A kinases. It is noteworthy that DYRK1A received recently much attention due to its implication in the development of sporadic Alzheimer's disease [18,19] and Down syndrome [20,21], where it promotes neurodegeneration by hyperphosphorylation of the microtubule-associated protein tau. CLKs share a strong structural homology and some physiological functions with the DYRKs family [22]. CLK1 is also involved in the pathophysiology of Alzheimer's disease by phosphorylating the serine residue in serine and arginine-rich proteins. Hence, the inhibition of DYRK1A and CLK1 may be used as a therapeutic strategy for Alzheimer's disease and related disorders [22].

Imidazo[1,2-*a*]pyridines exhibit a broad range of biological proprieties [23–25] including antiviral [26], anticancer [27,28], antifungal [29], anti-inflammatory activities [30] and they have also been incorporated into compounds useful for imaging Aβ aggregates in patients with Alzheimer's disease [31,32].

Due to the biological importance of these compounds, we aimed to investigate new representatives on imidazo[1,2-*a*]pyridines heterocyclic scaffold able to modulate a kinase activity. To optimize the potency of this analogous and to gain further insight into its structure–activity relationships (SARs), we designed and synthesized several new imidazo[1,2-*a*]pyridine derivatives with modification on the nucleus A or on ring B (Fig. 1).

2. Results and discussion

2.1. Chemistry

A series of 6- or 2-substituted imidazo[1,2-*a*]pyridines (Tables 1 and 2) were prepared from a variety of commercially available 5-substituted 2-aminopyridines with 5-(2-bromoacetyl)-2-hydroxybenzamide derivatives. In a single step a large variety of imidazo[1,2-*a*]pyridines bearing various substituents was readily obtained [33,34].

In order to optimize the synthetic procedure, we used 5-(2-bromoacetyl)-2-hydroxybenzamide **6a** and 5-chloro-2-aminopyridin **5a** as a model system (Table 1, entry 1). Reacting 1 equiv. of **5a** with 1.05 equiv. of **6a** in the presence of 2 equiv. of K_2CO_3 in EtOH [35] gave **4a** with a yield of 31%. The influence of different mineral bases on reaction yield was investigated, with sodium bicarbonate ($NaHCO_3$) proving optimal, giving **4a** in an improved yield of 65% (Table 1, entry 1).

With this modified conditions, we prepared a small library of imidazo[1,2-*a*]pyridines varying the substituents on ring A. Halogenated imidazo[1,2-*a*]pyridines (entries 1–4) were obtained in moderate yield ranging from 30 to 75% with the highest yield arising with unsubstituted aminopyridine (entry 5). A decrease in the yield was noticed in the case of analogues bearing an electron donating or hydrogen-bond donating group at the 5-position (entries 6 and 7).

Table 3
Kinase inhibitory activity of imidazo[1,2-*a*]pyridines derivatives.[a,b]

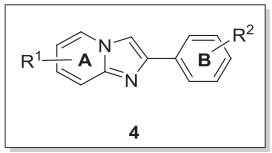

4

Compound	CK1	GSK-3	DYRK1A	CLK1	Compound	CK1	GSK-3	DYRK1A	CLK1
4a	NA[d]	NA[d]	**8.9**	**1.4**	**4k**	NA[d]	NA[d]	NA[d]	NA[d]
4b	NA[d]	NA[d]	4.7	1.4	**4l**	NA[d]	NA[d]	NA[d]	NA[d]
4c	NA[d]	NA[d]	**2.6**	**0.7**	**4m**	NA[d]	NA[d]	NA[d]	NA[d]
4d	NA[d]	NA[d]	NA[d]	NA[d]	**4n**	NA[d]	NA[d]	NA[d]	NA[d]
4e	NA[d]	NA[d]	**4**	**1**	**4o**	NA[d]	NA[d]	NA[d]	NA[d]
4f	NA[d]	NA[d]	**3**	**0.89**	**4p**	NA[d]	NA[d]	NA[d]	NA[d]
4g	NA[d]	NA[d]	NA[d]	NA[d]	**4q**	NA[d]	NA[d]	NA[d]	NA[d]
4h	NA[d]	NA[d]	NA[d]	NA[d]	**4r**	NA[d]	NA[d]	NA[d]	NA[d]
4i	NA[d]	NA[d]	NA[d]	NA[d]	Harmine	1.50	>10	0.029	0.072
4j	NA[d]	NA[d]	6	1.7	Leucettine L41[c]	–	0.040	0.040	0.090

[a] IC_{50} values are reported in μM. The most significant results are presented in bold.
[b] Kinases activities were assayed in triplicate. Typically, the standard deviation of single data points was below 10%.
[c] Leucettine L41 (IC_{50} in μM) [12,37].
[d] NA, not active. A compound was considered as not active (NA) when its inhibitory activity on kinases showing less than 50% inhibition (IC_{50} > 10 μM).

For studies investigating modification on ring B, 5-chloro-2-aminopyridin **5a** was used as the amine partner, with the variation of the nature of the 2-bromoacetophenone **6**. The imidazo[1,2-*a*]pyridines (**4k-4r**) were obtained using the conditions described above in modest yield (10–62%) to provide a library of 18 novel compounds.

2.2. Biological results

In our screening efforts to discover new scaffolds for the inhibition of disease-relevant protein kinases, we initially screened a library of over 110 low molecular weight compounds against the kinases DYRK1A and CLK1. This library comprised numerous synthetic products including molecules containing imidazo [1,2-*a*] pyridines ring. Among these, compound **4a** was found to be a modest but significant inhibitor of these disease-associated kinases.

Thereafter, the synthetic imidazo [1,2-*a*]pyridines derivatives **4a-r** were thus tested on a small panel of four kinases: (i) CK1δ/ε (casein kinase 1); (ii) GSK-3α/β (Glycogen Synthase Kinase-3α/β); (iii) DYRK1A; (iv) CLK1. All compounds were first tested at a final concentration of 10 μM. Those showing less than 50% inhibition were considered as inactive (IC_{50} > 10 μM). Compounds displaying more than 50% inhibition at 10 μM were next tested over a wide range of concentrations (usually 0.01–10 μM) and IC_{50} values were determined from the dose response curves (Sigma-Plot). The results of the *in vitro* kinase assay were summarized in Table 3.

Among the compounds tested, besides the first identified compound **4a**, the three most interesting molecules are **4c**, **4e** and **4f** which micromolar activities against DYRK1A (2.6 μM ≤ IC_{50} ≤ 4 μM) and submicromolar IC_{50} values against CLK1 (0.7 μM ≤ IC_{50} ≤ 1 μM). **4b** and **4j** are a slightly less active against DYRK1A (4.7 μM ≤ IC_{50} ≤ 6 μM) and CLK1 (1.4 μM ≤ IC_{50} ≤ 1.7 μM) and no activity was observed for the other compounds of the series. This appears to define a specific role of the aromatic substituents in the 6-position of imidazo[1,2-*a*]pyridines, indicating that this aromatic ring substituted by a hydroxyl group in position 4′ and a carboxamide at 5′ position. Replacement of these substituents by a methoxy or amino group (**4k-4r**) leads to a loss of the inhibitory activity against CLK1 and DYRK1A. Nevertheless, the 6-position of imidazo[1,2-*a*]pyridines tolerated various substituents such as chlorine, fluorine, bromine, hydrogen and hydroxyl (**4a-c**, **4e**, and **4f**). The imidazo[1,2-*a*]pyridine scaffold could be successfully replaced by an imidazo[1,2-*a*]pyrazine core (compound **4j**) and retain similar kinase inhibition activity. The introduction of bulky phenyl substituent (**4h** and **4i**) at the 6-position of imidazo[1,2-*a*] pyridine was unfavorable for compound **4** activity. Imidazo[1,2-*a*] pyridine compounds (**4c**, **4e,** and **4f**) were less potent in comparison with harmine and leucettine L41 against DYRK1A and CLK1 [36]. However, they constituted a promising starting point for the

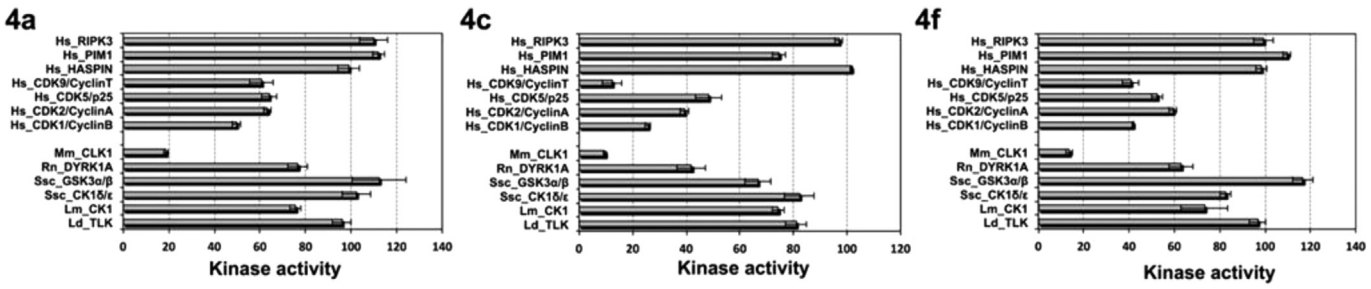

Fig. 2. Inhibitory activity of **4a, 4c and 4f** against a panel of 13 protein kinases. Kinase activities in the presence of 10 μM of compound are presented as % of maximal activity (i.e. measured in the absence of inhibitor). ATP concentration used in the kinase assays was 15 μmol/l n = 2 (mean ± range). Kinases are from human origin unless specified: *Ssc*, *Sus Scrofa*; *Rn*, *Rattus norvegicus*; *Mm*, *Mus musculus*; *Lm*, *Leishmania major*; Ld, *Leishmania donovani*.

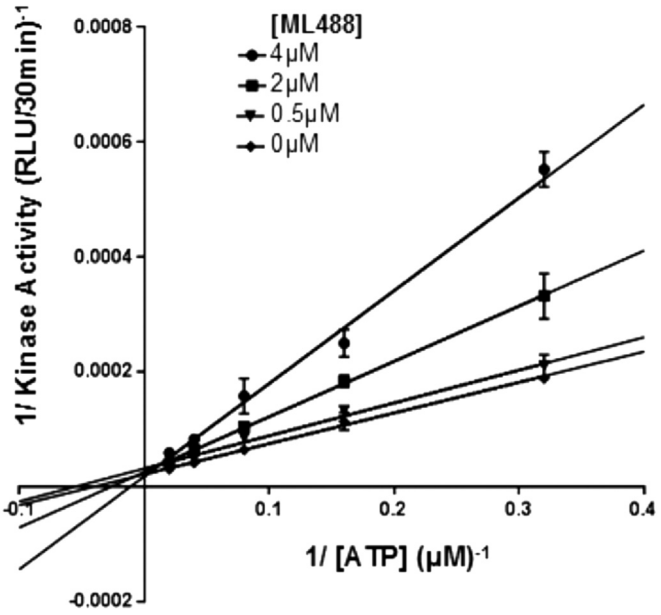

Fig. 3. Double reciprocal plots of the inhibition caused by **4c** compound on *Mm*CLK1. The experiment was carried out as described in material and methods section using a fixed concentration of substrate peptide (6.75 ng/μl) and ATP concentrations varying from 3.125 to 100 μM. Data are mean ± standard deviation, n = 3.

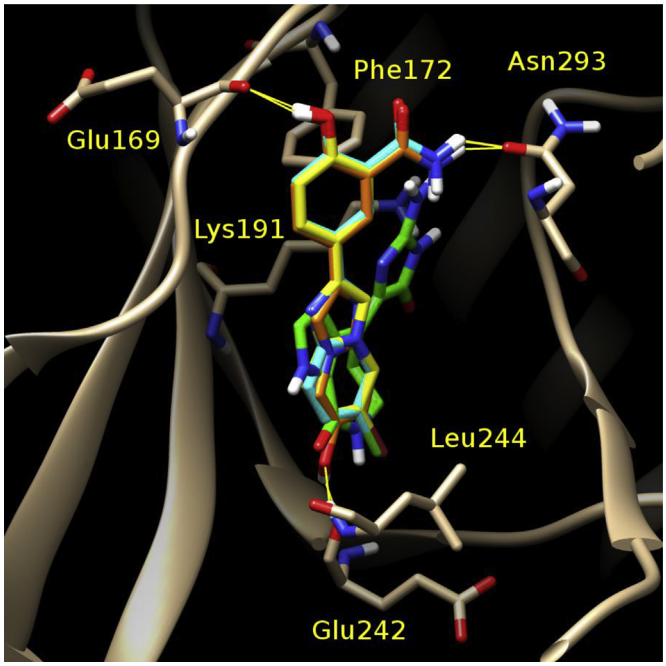

Fig. 4. Docking binding mode of compounds **4a** (cyan), **4c** (yellow) and **4f** (orange) over CLK1 (PDB: 1Z57) and superimposed to the co-crystallized hymenialdisine (HMD) (green). Important amino acid residues are labeled. Putative hydrogen bonding was depicted as yellow lines. Molecular graphics were performed with the UCSF Chimera package. (For interpretation of the references to colour in this figure legend, the reader is referred to the web version of this article.)

discovery of novel bioactive molecules, this study allows improved understanding SARs in this series which should enable the design of more efficient inhibitors of these disease-related kinases.

To confirm the selectivity of the more potent imidazo [1,2-*a*] pyridines **4a**, **4c** and **4f** derivatives toward DYRK1A and CLK1, we

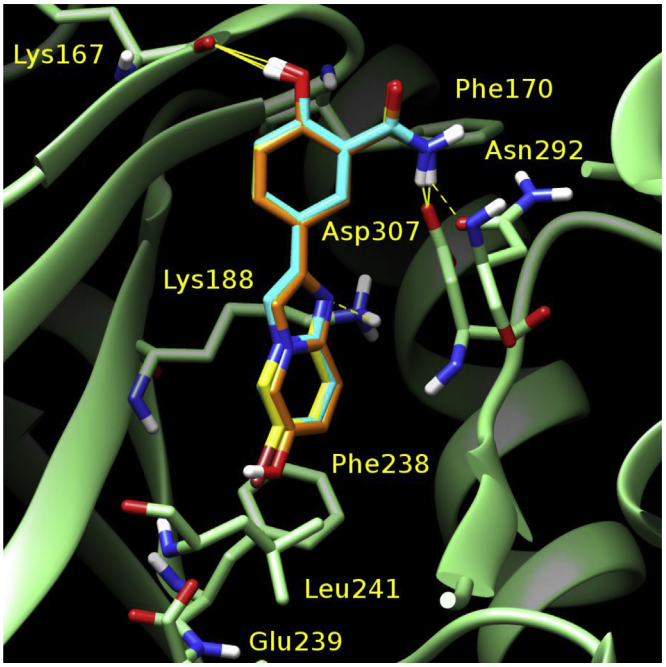

Fig. 5. Docking of compounds **4a** (cyan), **4c** (yellow) and **4f** (orange) on DYRK1 (PDB: 4MQ1). Important amino acid residues are labeled. Putative hydrogen bonding was depicted as yellow lines. Molecular graphics were performed using the UCSF Chimera package. The closest hydrogen bond complementary atom to side chain ammonium group of Lys188 and side chain carbonyl oxygen of Asn292 are indicated by dashed lines. (Distances are respectively 3.27 and 2.64 Å). (For interpretation of the references to colour in this figure legend, the reader is referred to the web version of this article.)

measured the inhibitory activity of this new molecule against a panel of 13 protein kinases (Fig. 2). The rational for testing these kinases is their involvement in human pathologies or disorders (notably in cancer). Some of these kinases are structurally related as they are members of the same group of the kinome [38]. In the tested panel, CDK1, 2, 5 and 9 are indeed members of the CMGC cluster (for CDK, MAPK, GSK3, and CLK). As reported in Fig. 2, members of this group are the more affected by the tested compounds, the greatest selectivity was obtained toward CLK1. Among the three active compounds, only, compound **4c** was moderately active against CDK9. Inhibitors of CDK9 can be used as an inductor of caspase-dependent apoptosis [39].

Studies to investigate the mechanism of kinase inhibition by this class of molecules were performed using compound **4c** and *Mm*CLK1, the more affected target of the panel. Kinetic experiments were performed by varying both ATP levels and **4c** concentrations (Fig. 3). Double-reciprocal plotting of the experimental data shows that **4c** is a typical ATP-competitive inhibitor for *Mm*CLK1.

2.3. Molecular modeling

Molecular docking was accomplished for compounds **4a**, **4c**, and **4f** in order to investigate their possible binding mode in the ATP binding site (as demonstrated by ATP competition assay, Fig. 3). These molecules were docked into the X-ray crystal structure of CLK1 (resolution = 1.7 Å) [40] and also into the DYRK1A (resolution = 2.35 Å) [41]. Both structures were retrieved from the Protein Data Bank (PDBs ID: 1Z57 and 4MQ1, respectively). The structure of the kinase inhibitor hymenialdisine (HMD) co-crystallized with CLK1 and of pyrido[2,3-*d*]pyrimidine co-crystallized with DYRK1A kinase was used as references in order to define the binding site cavity. Docking results on CLK1 showed

that all these three molecules present a partial superposition with the co-crystallized HMD (Fig. 4), and may form some similar hydrogen bonds interactions. The imidazo[1,2-*a*]pyridine cyclic systems of molecules **4a**, **4c** and **4f** are superposed to the pyrrolo [2,3-*c*]azepine of HMD. In **4f**, the hydroxyl from the imidazo[1,2-*a*] pyridine cycle establishes two hydrogen bonds with the backbone carbonyl of Glu242 and the NH of Leu244 as in the crystallized HMD. The chlorine atom of **4a** and the bromine atom of **4c** occupy the same region of space. These chlorine and bromine atoms are positioned close to the location occupied by a chlorine atom in ethyl 3-(2-amino-1-cyanoethenyl)-6,7-dichloro-1-methylindole-2-carboxylate (KHCB19) that has also been co-crystallized in the CLK1 kinase (PDB ID: 2VAG) (Supplementary material FS1) [42]. In both cases, the chlorine and bromide are placed at 2.7 Å from backbone carbonyl of Glu242 at the same position as the hydrogen bond donor of common kinase inhibitors, mimicking the NH_2 group of ATP. Although when halogen bonds are significantly weaker than hydrogen bonds their interactions can lead to establishing this conformation and to clear gains in binding affinity [43]. The hydroxybenzamide cycle, common to all the compounds, forms two hydrogen bonds with residues in the binding site. The amide NH_2 forms a hydrogen bond with the side chain carbonyl of Asn293, an amino acid also involved in the binding of HMD, and the phenol forms a hydrogen bonding interaction with the backbone carbonyl of Glu169 (Fig. 4). Finally, an edge-to-face t-stacking interaction occurs between the hydroxybenzamide cycle and Phe172 for all compounds.

Docking results on DYRK1A (Fig. 5) show again a very similar binding mode as in CLK1 kinase. However, the Phe170 in DYRK1A (Phe172 in CLK1) does not point inside the cavity and it is facing the outside of the loop. This opens the possibility for some different interactions between the compounds and the protein. The docking suggests that the nitrogen of the imidazo[1,2-*a*]pyridine cycle forms in all cases a hydrogen bond with Lys188 (Lys191 in CLK1). It should be noted that in CLK1, Lys191 also interacts with the co-crystallized HMD (not shown for clarity in Fig. 5) and KHCB19, via hydrogen bonds. However, in the case of CLK1, taking into account the presence of the Phe172, our molecules doesn't establish any interaction with this Lys191. When comparing the co-crystallized pyrido[2,3-*d*]pyrimidine in the DYRK1A kinase with our compounds, we find again a nice superposition especially around one of the chlorophenyl cycles and the imidazo[1,2-*a*]pyridine cycle (Supplementary material FS2). In this fitting, chlorine from the co-crystallized pyrido[2,3-*d*]pyrimidine and chlorine from **4a** as well as bromide from **4c**, can establish a halogen bond interaction with the carbonyl oxygen of Glu239 (Glu242 in CLK1 kinase). However, the hydroxyl group belonging to **4f** is located at the same position but doesn't appear to be able to establish any hydrogen bonding interaction with this carbonyl. As in CLK1, the hydroxybenzamide cycle forms two hydrogen bonds, one with Asp307 (Asp325 in CLK1 kinase that also participates in the binding of HMD), and a second one with the backbone carbonyl of Lys167 (Glu169 in CLK1 kinase) (Fig. 5).

The amide in the hydroxybenzamide cycle is positioned between the Asp307 and the Asn292 (Asn293 in CLK1 kinase) making possible hydrogen bonds interactions. Once more, a very good t-stacking interaction for all compounds is present but this time between the imidazo[1,2-*a*]pyridine cycle and Phe238, an interaction that is also present into the co-crystallized pyrido[2,3-*d*]pyrimidine compound. We have shown that the binding mode of our compounds shares several interactions with the same amino acids as the co-crystallized ligands of CLK1 and DYRK1A. The majority of kinase inhibitors known for CLK1 form a hydrogen bond to the backbone NH located at the center of the active site of the hinge strand as it is the case for our compounds. These results suggest a possible binding mode, but the docking results can't explain the very similar activity of these molecules. For instance, despite the fact that the hydroxyl group belonging to **4f** compound doesn't establish any hydrogen bonds interactions, a slight positive effect was observed for the inhibition of DYRK1A.

3. Conclusions

We have described the synthesis of a new series of imidazo[1,2-*a*]pyridine derivatives generated from 2-aminopyridine and 2-bromoacetophenone in a single reaction. Kinase assays determined that six of these molecules can inhibit the enzymatic activity of DYRK1A and CLK1 with IC_{50}s in a micromolar range. Compound **4c** was the most potent compound identified, with an IC_{50} of 0.7 μM against CLK1 and 2.6 μM against DYRK1A, and may provide a new lead compound for molecular targeted drug discovery. Molecular modeling studies and kinetic experiments have shown that molecules **4a**, **4c**, and **4f** have a good fit well in the ATP binding site of these disease-related kinases, and are able to establish several hydrogen bonds with critical residues in the ATP-binding site of these targets. Interestingly, CDK5/p25 (Cyclin-dependent kinase 5), one of the major tau kinase associated with neurodegenerative disease [44], is poorly affected by **4a**, **4c**, and **4f**. Further chemical modifications of the structure may extend the selectivity profile. Inhibition of kinases CLK1, DYRK1A, and CDK5 by such multi-target compounds may produce synergistic therapeutic effects. These results constitute a starting point enabling a better understanding of structure-activity relationships of this new series of compounds, and should facilitate future elaboration to more efficient and selective inhibitors of DYRK1A and CLK1 which may have applications in affecting the pathogenesis of Alzheimer's disease and related disorders including Down's syndrome.

4. Experimental

4.1. Chemistry

4.1.1. General considerations

Melting points (mp) were recorded on a Büchi B-450 apparatus and were uncorrected. NMR spectra were performed on a Bruker AVANCE 300. Chemical shifts δ are given in ppm, and the following abbreviations are used: singlet (s), doublet (d), doublet of doublet (dd), triplet (t), multiplet (m) and broad singlet (brs). IR spectra were measured on a Bruker Vector 22 spectrophotometer (neat, cm^{-1}). Low-resolution mass spectra (*m*/*z*) were recorded on a Bruker Esquire electrospray ionization apparatus. High-resolution mass spectra were recorded on a MicrotofQ Bruker Daltonics. Reaction courses and product mixtures were routinely monitored by TLC on silica gel (precoated F254 Merck plates), and compounds were visualized with under a UVP Mineralight UVGL-58 lamp (254 nm) and with phosphomolybdic acid, *p*-anisaldehyde, or vanillin. Flash chromatography was performed using silica gel 60 (40–63 mm, 230–400 mesh ASTM) at medium pressure (200 mbar). Organic extracts were dried over magnesium sulfate. All products reported showed ^1H NMR spectra in agreement with the assigned structures.

4.1.2. General procedure for the synthesis of imidazo [1,2-a] pyridines

A mixture of 2-bromoacetophenone **6** (1.05 mmol), 2-aminopyridine **5** (1.0 mmol) and $NaHCO_3$ (2.0 mmol) in EtOH (20 mL) was refluxed overnight. After cooling, the mixture was evaporated to dryness and the residue was taken up with H_2O. The aqueous solution was acidified with 3 N HCl and the insoluble solid was filtered off. The filtrate was basified with aqueous 5% NaOH and

extracted with dichloromethane (3 × 20 mL). The collected organic layers were dried over Na_2SO_4 and evaporated under reduced pressure. The crude residue was purified by flash chromatography on silica gel using a mixture of dichloromethane/ethyl acetate as eluent to afford the compound **4.**

4.1.3. 5-(6-Chloroimidazo [1,2-a]pyridin-2-yl)-2-hydroxybenzamide (4a)

Yield 65%; yellow solid; mp: 274–275 °C; ^{1}H NMR (300 MHz, DMSO-d_6) δ 13.13 (s, 1H, OH), 8.89 (dd, J = 2.1, 1 Hz, 1H, Ar), 8.59 (s, 1H, CONH), 8.46 (d, J = 2.1 Hz, 1H, Ar), 8.26 (s, 1H, Ar), 8.03 (dd, J = 8.6, 2.1 Hz, 1H, Ar), 7.97 (s, 1H, CONH), 7.61 (d, J = 9.6 Hz, 1H, Ar), 7.29 (dd, J = 9.6, 2.1 Hz, 1H, Ar), 6.98 (d, J = 8.6 Hz, 1H, Ar); ^{13}C NMR (75 MHz, DMSO-d_6) δ 171.9 (CO), 160.9 (C), 145.2 (C), 143.2 (C), 131.4 (CH), 125.5 (2 CH), 124.7 (CH), 124.2 (C), 118.8 (C), 117.8 (CH), 117.0 (CH), 114.6 (C), 108.8 (CH); IR (ν, cm^{-1}):3454 (O–H), 3429, 3400 (NH amide), 3331, 3192, 3135, 2949, 2340, 2121, 2292, 2064, 2033, 2012, 1073; HMRS: found (ESI +) m/z 288.0538, calcd for $C_{14}H_{11}ClN_3O_2$ (M+H)$^+$: 288.0538.

4.1.4. 5-(6-Fluoroimidazo [1,2-a]pyridin-2-yl)-2-hydroxybenzamide (4b)

Yield 35%; white solid; mp: 288–289 °C; ^{1}H NMR (300 MHz, DMSO-d_6) δ 13.10 (s, 1H), 8.83–8.76 (m, 1H), 8.58 (s, 1H), 8.45 (d, J = 2.1 Hz, 1H), 8.27 (s, 1H), 8.01 (dd, J = 8.6, 2.1 Hz, 1H), 7.95 (s, 1H), 7.61 (dd, J = 9.8, 5.3 Hz, 1H), 7.36–7.24 (m, 1H), 6.96 (d, J = 8.6 Hz, 1H); ^{13}C NMR (75 MHz, DMSO-d_6) δ 177.1, 166.1, 157.8 (d, J = 230 Hz), 150.7, 147.9, 136.5, 130.6, 129.6, 123.0, 122.2 (d, J = 9 Hz), 121.6 (d, J = 22.5 Hz), 119.9, 118.8 (d, J = 22.5 Hz), 114.9; ^{19}F NMR (188 MHz, DMSO) δ −139.94; IR (ν, cm^{-1}): 3435, 3429, 2361, 2202, 1678, 1603, 1568, 1535, 1477, 1369, 1255, 1207, 1169; HMRS: found (ESI +) m/z 272.0833, calcd for $C_{14}H_{11}FN_3O_2$ (M+H)$^+$: 272.0835.

4.1.5. 5-(6-Bromoimidazo [1,2-a]pyridin-2-yl)-2-hydroxybenzamide (4c)

Yield 40%; yellow solid; mp: 254–255 °C; ^{1}H NMR (300 MHz, DMSO-d_6) δ 13.13 (s, 1H), 9.01–8.85 (m, 1H), 8.60 (s, 1H), 8.44 (d, J = 2.1 Hz, 1H), 8.23 (s, 1H), 8.00 (dd, J = 8.6, 2.1 Hz, 1H), 7.97 (s, 1H), 7.53 (d, J = 9.5 Hz, 1H), 7.34 (dd, J = 9.5, 2.1 Hz, 1H), 6.95 (d, J = 8.6 Hz, 1H); δ ^{13}C NMR (75 MHz, DMSO-d_6) δ 171.9, 161.0, 144.9, 143.2, 131.4, 127.7, 126.9, 125.5, 124.2, 117.8, 117.3, 114.6, 108.6, 105.8; IR (ν, cm^{-1}):2361, 2341, 1671, 1624, 1590, 1516, 1472, 1441, 1336, 1283, 1140, 1059; HMRS: found (ESI +) m/z 332.0033, calcd for $C_{14}H_{11}BrN_3O_2$ (M+H)$^+$: 332.0035.

4.1.6. 5-(6-Iodoimidazo [1,2-a]pyridin-2-yl)-2-hydroxybenzamide (4d)

Yield 30%; yellow solid; mp: 181–182 °C; ^{1}H NMR (300 MHz, DMSO-d_6) δ 13.12 (s, 1H), 8.95 (s, 1H), 8.60 (s, 1H), 8.43 (d, J = 2.0 Hz, 1H), 8.19 (s, 1H), 7.99 (dd, J = 8.6, 2.0 Hz, 1H), 7.98 (s, 1H), 7.40 (d, J = 0.9 Hz, 2H), 6.95 (d, J = 8.6 Hz, 1H); ^{13}C NMR (75 MHz, DMSO-d_6) δ 171.9, 160.9, 144.4, 143.3, 132.3, 131.4, 131.4, 125.5, 124.2, 117.8, 117.6, 114.6, 108.0, 75.9; IR (ν, cm^{-1}):3425, 3347, 3217, 2483, 2207, 2166, 2028, 2011, 1482; HMRS: found (ESI +) m/z 379.9896, calcd for $C_{14}H_{11}IN_3O_2$ (M+H)$^+$: 379.9896.

4.1.7. 5-(Imidazo [1,2-a]pyridin-2-yl)-2-hydroxybenzamide (4e)

Yield 75%; yellow solid; mp: 238–239 °C; ^{1}H NMR (300 MHz, DMSO-d_6) δ 13.89 (s, 1H), 9.38 (s, 1H), 9.33 (d, J = 6.7 Hz, 1H), 9.27 (d, J = 2.1 Hz, 1H), 9.05 (s, 1H), 8.81 (dd, J = 8.6, 2.1 Hz, 1H), 8.75 (s, 1H), 8.34 (d, J = 9.1 Hz, 1H), 8.01 (ddd, J = 9.1, 6.7, 1.2 Hz, 1H), 7.76 (d, J = 8.6 Hz, 1H), 7.66 (td, J = 6.7, 1.2 Hz, 1H); ^{13}C NMR (75 MHz, DMSO-d_6) δ 172.0, 160.7, 144.7, 144.2, 131.3, 126.8, 125.4, 124.7, 124.7, 117.7, 116.3, 114.6, 112.1, 108.1; IR (ν, cm^{-1}):3427, 3347, 3215, 2483, 2208, 2167, 1665, 1629, 1590, 1429, 1370, 1278, 1127, 1075; HMRS: found (ESI +) m/z 254.0935, calcd for $C_{14}H_{12}N_3O_2$ (M+H)$^+$: 254.0936.

4.1.8. 2-Hydroxy-5-(6-hydroxyimidazo [1,2-a]pyridin-2-yl) benzamide (4f)

Yield 16%; white solid; mp: 190–191 °C; ^{1}H NMR (300 MHz, MeOD) δ 8.30 (d, J = 2.1 Hz, 1H), 8.00 (s, 1H), 7.94 (dd, J = 8.6, 2.2 Hz, 2H), 7.43 (d, J = 9.6 Hz, 1H), 7.07 (dd, J = 9.6, 2.2 Hz, 1H), 7.00 (d, J = 8.6 Hz, 1H); ^{13}C NMR (75 MHz, Acetone-$d6$) δ 174.1, 162.8, 146.8, 132.6, 132.2, 126.4, 125.5, 121.0, 120.5, 118.9, 117.6, 114.9, 111.2, 109.2; IR (ν, cm^{-1}):2384, 2218, 1609, 1333, 1255, 1176, 1125, 1075; HMRS: found (ESI +) m/z 270.0883, calcd for $C_{14}H_{12}N_3O_3$ (M + H)$^+$: 270.0879.

4.1.9. 5-(6-Aminoimidazo [1,2-a]pyridin-2-yl)-2-hydroxybenzamide (4g)

Yield 8%; pink solid; mp: 186–187 °C; ^{1}H NMR (400 MHz, Acetone-d_6) δ 11.22 (s, 1H), 8.63 (d, J = 7.8 Hz, 1H), 8.55–8.42 (m, 1H), 8.35 (d, J = 2.6 Hz, 1H), 8.25 (d, J = 8.0 Hz, 1H), 8.02–7.83 (m, 3H), 3.58 (s, 4H); ^{13}C NMR (101 MHz, Acetone-$d6$) δ 163.2, 138.2, 133.8, 133.2, 130.5, 129.4, 126.5, 125.7, 123.6, 122.6, 120.7, 119.9, 116.1, 112.7; IR (ν, cm^{-1}): 2989, 2960, 2361, 1676, 1624, 1594, 1594, 1494, 1411, 1362, 1275, 1115, 1062, 1034; HMRS: found (ESI +) m/z 269.1041, calcd for $C_{14}H_{13}N_4O_2$ (M + H)$^+$: 269.1039.

4.1.10. 2-Hydroxy-5-(6-(4-methoxyphenyl)imidazo [1,2-a]pyridin-2-yl)benzamide (4h)

Yield 50%; pink solid; mp: 245–246 °C; ^{1}H NMR (300 MHz, DMSO-d_6) δ 13.11 (s, 1H), 8.82 (d, J = 1.6 Hz, 1H), 8.61 (s, 1H), 8.48 (d, J = 2.0 Hz, 1H), 8.26 (s, 1H), 8.03 (dd, J = 8.6, 2.0 Hz, 1H), 7.95 (s, 1H), 7.68–7.63 (m, 2H), 7.61 (d, J = 9.3 Hz, 1H), 7.54 (dd, J = 9.4, 1.8 Hz, 1H), 7.10–7.03 (m, 2H), 6.97 (d, J = 8.6 Hz, 1H), 3.81 (s, 3H); ^{13}C NMR (75 MHz, DMSO-d_6) δ 172.0, 160.7, 159.0, 144.5, 143.9, 131.3, 128.9, 127.7, 127.7, 125.3, 124.9, 124.7, 124.7, 123.1, 117.7, 116.2, 114.6, 114.5, 114.5, 108.5, 55.2; IR (ν, cm^{-1}):3418, 3253, 2277, 2361, 2207, 2149, 2013, 1998, 1632, 1405, 1242, 1181, 1017; HMRS: found (ESI +) m/z 360.1366, calcd for $C_{21}H_{18}N_3O_3$ (M + H)$^+$: 360.1363.

4.1.11. 2-Hydroxy-5-(6-(4-nitrophenyl)imidazo [1,2-a]pyridin-2-yl) benzamide (4i)

Yield 25%; pink solid; mp: 148–149 °C; ^{1}H NMR (300 MHz, DMSO-d_6) δ 13.13 (s, 1H), 9.13 (s, 1H), 8.61 (s, 1H), 8.48 (dd, J = 11.6, 2.0 Hz, 1H), 8.37 (s, 1H), 8.33 (d, J = 4.0 Hz, 2H), 8.06 (dd, J = 8.5, 2.1 Hz, 2H), 8.05 (d, J = 8.9 Hz, 2H), 7.97 (s, 1H), 7.70 (d, J = 1.0 Hz, 1H), 6.99 (d, J = 8.6 Hz, 1H); ^{13}C NMR (75 MHz, DMSO-d_6) δ 171.9, 161.2, 160.9, 152.5, 146.7, 145.2, 144.2, 143.4, 131.4, 127.5, 127.5, 125.6, 125.5, 124.2, 124.2, 122.9, 117.8, 116.6, 114.6, 108.9; IR (ν, cm^{-1}):2926, 2853,2360, 1658, 1592, 1471, 1376, 1247, 1109, 1034; HMRS: found (ESI +) m/z 375.1102, calcd for $C_{20}H_{15}N_4O_4$ (M + H)$^+$: 375.1093.

4.1.12. 2-Hydroxy-5-(imidazo [1,2-a]pyrazin-2-yl)benzamide (4j)

Yield 12%; yellow solid; mp: 264–265 °C; ^{1}H NMR (300 MHz, DMSO-d_6) δ 9.04 (s, 1H), 8.64 (d, J = 4.5 Hz, 1H), 8.54 (d, J = 1.9 Hz, 1H), 8.46 (s, 1H), 8.08 (d, J = 10.6 Hz, 1H), 7.89 (d, J = 4.6 Hz, 1H), 7.00 (d, J = 8.6 Hz, 1H); ^{13}C NMR (75 MHz, DMSO-d_6) δ 171.8, 161.3, 146.0, 142.1, 140.3, 134.6, 131.6, 130.4, 129.1, 126.0, 123.7, 117.9, 114.7; IR (ν, cm^{-1}): 3396, 2360, 1707, 1669, 1593, 1493, 1283, 1237, 1037, 1022; HMRS: found (ESI +) m/z 255.0883, calcd for $C_{13}H_{11}N_4O_2$ (M + H)$^+$: 255.0882.

4.1.13. 3-(6-Chloroimidazo [1,2-a]pyridin-2-yl)benzamide (4k)

Yield 20%; brownish solid; mp: 176–177 °C; ^{1}H NMR (300 MHz, Acetone-$d6$): 8.76–8.71 (m, 1H), 8.67 (s, 1H), 8.60 (td, J = 1.7, 0.6 Hz, 1H), 8.41–8.30 (m, 3H), 8.30–8.20 (m, 2H), 7.80–7.73 (m, 1H), 7.70

(s, 1H); ^{13}C NMR (75 MHz, DMSO-d_6) δ 192.2, 166.7, 166.5, 137.2, 134.7, 134.1, 133.5, 132.4, 131.5, 130.0, 129.6, 129.2, 128.6, 128.3; IR (ν, cm^{-1}): 3398, 2260, 1715, 1669, 1583, 1288, 1247, 1047, 1021; HMRS: found (ESI +) *m/z* 272.0595, calcd for $C_{14}H_{11}ClN_3O$ $(M + H)^+$: 272.0591.

4.1.14. 2-Bromo-4-(6-chloroimidazo [1,2-a]pyridin-2-yl)aniline ***(4l)***

Yield 40%; orange solid; mp: 227–228 °C; ^{1}H NMR (300 MHz, DMSO-d_6) δ 8.76 (dd, *J* = 2.0, 0.7 Hz, 1H), 8.21 (s, 1H), 7.97 (d, *J* = 1.9 Hz, 1H), 7.66 (dd, *J* = 8.4, 2.0 Hz, 1H), 7.57 (d, *J* = 9.5 Hz, 1H), 7.26 (dd, *J* = 9.5, 2.1 Hz, 1H), 6.87 (d, *J* = 8.4 Hz, 1H), 5.51 (s, 2H); ^{13}C NMR (75 MHz, DMSO-d_6) δ 145.7, 145.0, 143.1, 129.4, 125.9, 125.2, 124.4, 122.9, 118.6, 116.9, 115.4, 108.1, 107.5; IR (ν, cm^{-1}): 2924, 1619, 1554, 1480, 1406, 1336, 1220, 1156, 1072, 1033; HMRS: found (ESI +) *m/z* 323.9738, calcd for $C_{13}H_{10}ClN_3$ $(M + H)^+$: 323.9741.

4.1.15. 4-(6-Chloroimidazo [1,2-a]pyridin-2-yl)phenol ***(4m)***

Yield 22%; yellow solid; mp: 257–258 °C; ^{1}H NMR (300 MHz, DMSO-d_6) δ 9.58 (s, 1H), 8.74 (dd, *J* = 2.1, 0.8 Hz, 1H), 8.16 (s, 1H), 7.74 (d, *J* = 8.6 Hz, 2H), 7.54 (d, *J* = 9.5 Hz, 1H), 7.22 (dd, *J* = 9.5, 2.1 Hz, 1H), 6.80 (d, *J* = 8.6 Hz, 2H); ^{13}C NMR (75 MHz, DMSO-d_6) δ 157.5, 145.9, 143.1, 127.1, 127.1, 125.2, 124.5, 124.4, 118.6, 117.0, 115.5, 115.5, 108.2; IR (ν, cm^{-1}):2959, 2928, 2364, 1729, 1683, 1601, 1502, 1423, 1237, 1169, 1113, 1077; HMRS: found (ESI +) *m/z* 245.0471, calcd for $C_{13}H_{10}ClN_2O$ $(M + H)^+$: 245.0482.

4.1.16. 6-Chloro-2-(4-methoxyphenyl)imidazo [1,2-a]pyridine ***(4n)***

Yield 10%; yellow solid; mp: 231–233 °C; ^{1}H NMR (300 MHz, DMSO-d_6) δ 8.78 (dd, *J* = 2.1, 0.8 Hz, 1H), 8.27 (s, 1H), 7.89 (d, *J* = 8.9 Hz, 2H), 7.60 (d, *J* = 9.6 Hz, 1H), 7.27 (dd, *J* = 9.6, 2.1 Hz, 1H), 7.01 (d, *J* = 8.9 Hz, 2H), 3.80 (s, 3H); ^{13}C NMR (75 MHz, DMSO-d_6) δ 159.2, 145.5, 143.2, 127.0, 127.0, 126.0, 125.4, 124.6, 118.7, 117.1, 114.2, 114.2, 108.7, 55.1; IR (ν, cm^{-1}):3003, 1612, 1553, 1503, 1486, 1434, 1369, 1277, 1106, 1074, 1032; HMRS: found (ESI +) *m/z* 259.0631, calcd for $C_{14}H_{12}ClN_2O$ $(M + H)^+$: 259.0638.

4.1.17. 6-Chloro-2-(3-methoxyphenyl)imidazo [1,2-a]pyridine ***(4o)***

Yield 62%; yellow solid; mp: 145–146 °C; ^{1}H NMR (300 MHz, DMSO-d_6) δ 8.80 (dd, *J* = 2.1, 0.8 Hz, 1H), 8.39 (s, 1H), 7.64 (d, *J* = 9.6 Hz, 1H), 7.57–7.49 (m, 2H), 7.35 (t, *J* = 8.1 Hz, 1H), 7.29 (dd, *J* = 9.6, 2.1 Hz, 1H), 6.91 (ddd, *J* = 8.1, 2.1, 0.8 Hz, 1H), 3.83 (s, 3H); ^{13}C NMR (75 MHz, $CDCl_3$) δ 159.6, 145.2, 143.2, 134.8, 129.9, 125.8, 124.8, 119.0, 118.0, 117.4, 113.9, 110.7, 110.0, 55.1; IR (ν, cm^{-1}): 2835, 2360, 1613, 1521, 1469, 1367, 1314, 1253, 1197, 1074, 1046; HMRS: found (ESI +) *m/z* 259.0631, calcd for $C_{14}H_{12}ClN_2O$ $(M + H)^+$: 259.0638.

4.1.18. 6-Chloro-2-(3,5-dimethoxyphenyl)imidazo [1,2-a]pyridine ***(4p)***

Yield 46%; yellow solid; mp: 133–134 °C; ^{1}H NMR (300 MHz, Acetone-*d6*) δ 9.07 (dd, *J* = 2.0, 0.9 Hz, 1H), 8.75 (d, *J* = 0.5 Hz, 1H), 8.01 (d, *J* = 9.6 Hz, 1H), 7.69 (dd, *J* = 9.6, 2.0 Hz, 1H), 7.66 (d, *J* = 2.3 Hz, 2H), 6.92 (t, *J* = 2.3 Hz, 1H), 4.30 (s, 6H); ^{13}C NMR (75 MHz, Acetone-*d6*) δ 162.3, 162.3, 147.3, 144.7, 136.9, 126.5, 125.5, 120.6, 118.6, 110.9, 104.8, 104.8, 101.1, 55.8, 55.8; IR (ν, cm^{-1}):2838, 2361, 1611, 1543, 1457, 1418, 1341, 1288, 1204, 1154, 1073, 1049; HMRS: found (ESI +) *m/z* 289.0743, calcd for $C_{15}H_{14}ClN_2O_2$ $(M + H)^+$: 289.0744.

4.1.19. 6-Chloro-2-(3,5-dimethoxyphenyl)imidazo [1,2-a]pyridine ***(4q)***

Yield 40%; yellow solid; mp: 131–132 °C; ^{1}H NMR (300 MHz, $CDCl_3$) δ 8.15 (dd, *J* = 2.0, 0.8 Hz, 1H), 7.79 (s, 1H), 7.58 (d, *J* = 9.6 Hz, 1H), 7.16 (s, 2H), 7.13 (d, *J* = 2.0 Hz, 1H), 3.95 (s, 6H), 3.88 (s, 3H); ^{13}C NMR (75 MHz, $CDCl_3$) δ 153.8, 153.8, 146.6, 143.9, 138. 7, 128.7, 126.5, 123.5, 120.9, 117.7, 108.5, 103.5, 103.5, 61.1, 56.4, 56.4; IR (ν, cm^{-1}):2838, 1586, 1463, 1427, 1414, 1339, 1242, 1229, 1125, 1072, 1003; HMRS: found (ESI +) *m/z* 319.0850, calcd for $C_{16}H_{16}ClN_2O_3$ $(M + H)^+$: 319.0849.

4.1.20. 4-(6-Chloroimidazo [1,2-a]pyridin-2-yl)-2-methoxyphenol ***(4r)***

Yield 38%; yellow solid; mp: 205–206 °C; ^{1}H NMR (300 MHz, DMSO-d_6) δ 9.11 (s, 1H), 8.76 (dd, *J* = 2.0, 0.7 Hz, 1H), 8.19 (s, 1H), 7.58 (d, *J* = 9.6 Hz, 1H), 7.40 (d, *J* = 2.0 Hz, 1H), 7.35 (dd, *J* = 8.3, 2.1 Hz, 1H), 7.25 (dd, *J* = 9.6, 2.1 Hz, 1H), 6.97 (d, *J* = 8.3 Hz, 1H), 3.80 (s, 3H); ^{13}C NMR (75 MHz, DMSO-d_6) δ 147.8, 146.7, 145.7, 143.1, 126.4, 125.3, 124.5, 118.6, 117.1, 116.8, 113.0, 112.4, 108.7, 55.6; IR (ν, cm^{-1}):2364, 1557, 1469, 1423, 1338, 1264, 1246, 1223, 1173, 1132, 1073, 1013; HMRS: found (ESI +) *m/z* 275.0582, calcd for $C_{14}H_{12}ClN_2O_2$ $(M + H)^+$: 275.0587.

4.2. Kinase inhibition assay

Kinase activities were assayed in appropriate kinase buffer (A or B, described below), with either protein or peptide as substrate in the presence of 15 μM [γ-33P] ATP (3000 Ci/mmol; 10 mCi/ml) in a final volume of 30 μl following the assay described in Bach et al., [45]. Controls were performed with appropriate dilutions of dimethylsulfoxide. Full-length kinases are used unless specified. Peptide substrates were obtained from Proteogenix (Oberhausbergen, France).

Buffers:

(A) 10 mM MgCl2, 1 mM EGTA, 1 mM DTT, 25 mM Tris-HCl pH 7.5, 50 μg/ml heparin; (B) 60 mM β-glycerophosphate, 30 mM *p*-nitrophenyl-phosphate, 25 mM MOPS (pH 7), 5 mM EGTA, 15 mM MgCl2, 1 mM DTT, 0.1 mM sodium orthovanadate; (C) 60 mM β-glycerophosphate, 15 mM *p*-nitrophenyl-phosphate, 25 mM Mops (pH 7.2), 5 mM EGTA, 15 mM MgCl2, 1 mM DTT; (H) MOPS 25 mM pH 7.5, 10 mM MgCl2; (K) Tris 50 mM pH 7.5, 20 mM MgCl2, 2 mM MnCl2; (R) 5 mM MOPS pH 7.2, 2.5 mM β-glycerophosphate, 4 mM MgCl2, 2.5 mM MnCl2, 1 mM EGTA, 0.4 mM EDTA, 50 μg/ml BSA, 0.05 mM DTT; (G) Tris 40 mM pH 7.5, 20 mM MgCl2, 0.1 mg/ml BSA.

HsRIPK3 (human, recombinant, expressed by baculovirus in Sf9 insect cells) was assayed in buffer R with 0.1 μg/μl of MBP as substrate. HsPIM1 (human proto-oncogene, recombinant, expressed in bacteria) was assayed in buffer B with 0.8 μg/μl of histone H1 (Sigma #H5505) as substrate.

HsHaspin-kd (human, kinase domain, amino acids 470 to 798, recombinant, expressed in bacteria) was assayed in buffer H with 0.007 μg/μl of Histone H3 (1–21) peptide (ARTKQTARKSTGGKAPRKQLA) as substrate; HsCDK1/CyclinB1 (human, recombinant, expressed by baculovirus in Sf9 insect cells, SignalChem, product #C22-10G) was assayed in buffer G with 0.8 μg/μl of histone H1 as substrate.

HsCDK2/CyclinA (cyclin-dependent kinase-2, human, kindly provided by Dr. A. Echalier-Glazer, Leicester, UK) was assayed in buffer A (+0.15 mg/ml of BSA + 0.23 mg/ml of DTT) with 0.8 μg/μl of histone H1 as substrate.

HsCDK9/CyclinT (human, recombinant, expressed by baculovirus in Sf9 insect cells) was assayed in buffer A (+0.15 mg/ml of BSA + 0.23 mg/ml of DTT) with 0.27 μg/μl of the following peptide: YSPTSPSYSPTSPSYSPTSPSKKKK, as substrate.

HsCDK5/p25 (human, recombinant, expressed in bacteria) was assayed in buffer B, with 0.8 μg/μl of histone H1 as substrate.

SscGSK-3α/β (glycogen synthase kinase-3, porcine brain, native, affinity purified) was assayed in buffer A (+0.15 mg/ml of BSA + 0.23 mg/ml of DTT), with 0.010 μg/μl of GS-1 peptide, a GSK-3-selective substrate (YRRAAVPPSPSLSRHSSPHQSpEDEEE, "Sp"

stands for phosphorylated serine).

SscCK1δ/ε (casein kinase 1δ/ε, porcine brain, native, affinity purified) was assayed in buffer B, with 0.022 μg/μl of the following peptide: RRKHAAIGSpAYSITA as CK1-specific substrate.

RnDYRK1A-kd (Rattus norvegicus, amino acids 1 to 499 including the kinase domain, recombinant, expressed in bacteria, DNA vector kindly provided by Dr. W. Becker, Aachen, Germany) was assayed in buffer A (+0.5 mg/ml of BSA + 0.23 mg/ml of DTT) with 0.033 μg/μl of the following peptide: KKISGRLSPIMTEQ as substrate.

MmCLK1 (from Mus musculus, recombinant, expressed in bacteria) was assayed in buffer A (+0.15 mg/ml of BSA + 0.23 mg/ml of DTT) with 0.027 μg/μl of the following peptide: GRSRSRSRSRSR as substrate.

LdTLK (tousled-like kinase, from Leishmania donovani, recombinant, expressed in bacteria), was assayed in buffer K with 0.6 μg/μl of casein dephosphorylated from bovine milk (Sigma #C4032) as substrate.

LmCK1 (from Leishmania major, recombinant, expressed in bacteria) was assayed in buffer B (adjusted at pH 8) with 0.028 μg/μl of the following peptide: RRKHAAIGSpAYSITA as CK1-specific substrate.

4.2.1. ATP competition assay using ADP-GloTM bioluminescent assay

The activity of recombinant mouse CLK1 was measured using the ADP-GloTM bioluminescent kinase assay kit (Promega, Madison, WI) according to the recommendations of the manufacturer and described in Zegzouti et al., 2009 [46]. Reactions were carried out in a final volume of 5 μl for 30 min at 30 °C in ADP-Glo buffer (40 mM Tris pH 7.5, 20 mM $MgCl_2$ and 0.1 mg/ml of BSA). After that, 5 μl of ADP-GloTM Kinase Reagent was added to stop the kinase reaction. After an incubation time of 50 min at room temperature, 10 μl of Kinase Detection Reagent was added for 1 h at room temperature. The transmitted signal was measured using the Envision (PerkinElmer, Waltham, MA) microplate luminometer and expressed in Relative Light Unit (RLU). Assays were performed in the absence or presence of **4c** (4, 2 or 0.5 μM) and increasing concentrations of ATP (3.125–100 μM). The peptide: GRSRSRSRSRSR (6.75 ng/μl of reaction) was used as substrate. To plot and analyze the data Prism from GraphPad Software (La Jolla, CA) was used.

4.3. Molecular modeling

Coordinates for compounds **4a**, **4c** and **4f** were generated using CORINA v3.44 software [47]. Molecules were then docked in the ATP binding site from the CLK1 and DYRK1 kinases retrieved from the Protein Data Bank (PDBs ID: 1Z57 and 4MQ1, respectively), using GOLD v5.2.2 docking package software [48]. CHEMPLP with default parameters was used as an objective score function [49]. Structures of the complexes were exported for further examination and depiction with Chimera v1.9 software [50], including hydrogen bonds detection and close contact analysis.

Acknowledgments

The authors gratefully acknowledge the support of this project by CNRS, University Paris-Sud and “La Ligue Contre le Cancer” throughout an “Equipe Labellisée 2014” grant. We also thank the Cancéropôle Grand Ouest (axis: natural sea products in cancer treatment), IBiSA (French *Infrastructures en sciences du vivant: biologie, santé et agronomie*) and Biogenouest (Western France life science and environment core facility network) for supporting KISS*f* screening facility. S.B. is supported by ANR/Investissements d’Avenir program by means of the OCEANOMICs project (grant # ANR-11-BTBR-0008). Our laboratory (BioCIS UMR 8076) is a member of the laboratory of excellence LERMIT supported by a grant from ANR (ANR-10-LABX-33).

Appendix A. Supplementary data

Supplementary data related to this article can be found at http://dx.doi.org/10.1016/j.ejmech.2016.07.040.

References

[1] S. Cheek, H. Zhang, N.V. Grishin, Sequence and structure classification of kinases, J. Mol. Biol. 320 (2002) 855–881.
[2] S. Sharma, J. Singh, R. Ojha, H. Singh, M. Kaur, P.M.S. Bedi, K. Nepali, Design strategies, structure activity relationship and mechanistic insights for purines as kinase inhibitors, Eur. J. Med. Chem. 112 (2016) 298–346.
[3] Z.A. Stewart, M.D. Westfall, J.A. Pietenpol, Cell-cycle dysregulation and anticancer therapy, Trends Pharmacol. Sci. 24 (2003) 139–145.
[4] M.H. Flight, Neurodegenerative diseases: new kinase targets for Alzheimer's disease, Nat. Rev. Drug Discov. 12 (2013), 739–739.
[5] C.-H. Lin, Y.-S. Hsieh, Y.-R. Wu, C.-J. Hsu, H.-C. Chen, W.-H. Huang, K.-H. Chang, H.M. Hsieh-Li, M.-T. Su, Y.-C. Sun, G.-C. Lee, G.-J. Lee-Chen, Identifying GSK-3β kinase inhibitors of Alzheimer's disease: virtual screening, enzyme, and cell assays, Eur. J. Pharm. Sci. 89 (2016) 11–19.
[6] H. Noh, G.L. King, The role of protein kinase C activation in diabetic nephropathy, Kidney Int., 72(0000) S49–S53.
[7] S.K. Grant, Therapeutic protein kinase inhibitors, Cell. Mol. Life Sci. 66 (2009) 1163–1177.
[8] J. Zhang, P.L. Yang, N.S. Gray, Targeting cancer with small molecule kinase inhibitors, Nat. Rev. Cancer 9 (2009) 28–39.
[9] S. Sharma, S. Mehndiratta, S. Kumar, J. Singh, P.M.S. Bedi, K. Nepali, Purine analogues as kinase inhibitors: a review, Recent Pat. Anticancer Drug Discov. 10 (2015) 308–341.
[10] T. Herraiz, D. González, C. Ancín-Azpilicueta, V.J. Arán, H. Guillén, β-Carboline alkaloids in Peganum harmala and inhibition of human monoamine oxidase (MAO), Food Chem Toxicol. 48 (2010) 839–845.
[11] V. Samoylenko, M.M. Rahman, B.L. Tekwani, L.M. Tripathi, Y.-H. Wang, S.I. Khan, I.A. Khan, L.S. Miller, V.C. Joshi, I. Muhammad, Banisteriopsis caapi, a unique combination of MAO inhibitory and antioxidative constituents for the activities relevant to neurodegenerative disorders and Parkinson's disease, J. Ethnopharmacol. 127 (2010) 357–367.
[12] M. Debdab, F. Carreaux, S. Renault, M. Soundararajan, O. Fedorov, P. Filippakopoulos, O. Lozach, L. Babault, T. Tahtouh, B. Baratte, Y. Ogawa, M. Hagiwara, A. Eisenreich, U. Rauch, S. Knapp, L. Meijer, J.-P. Bazureau, Leucettines, a class of potent inhibitors of cdc2-like kinases and dual specificity, tyrosine phosphorylation regulated kinases derived from the marine sponge leucettamine b: modulation of alternative Pre-RNA splicing, J. Med. Chem. 54 (2011) 4172–4186.
[13] G.W. Chan, S. Mong, M.E. Hemling, A.J. Freyer, P.H. Offen, C.W. DeBrosse, H.M. Sarau, J.W. Westley, New leukotriene B4 receptor antagonist: leucettamine a and related imidazole alkaloids from the marine sponge leucetta microraphis, J. Nat. Prod. 56 (1993) 116–121.
[14] A. Bruel, C. Logé, M.-L.D. Tauzia, M. Ravache, R. Le Guevel, C. Guillouzo, J.-F. Lohier, J.S.-D. Oliveira Santos, O. Lozach, L. Meijer, S. Ruchaud, H. Bénédetti, J.-M. Robert, Synthesis and biological evaluation of new 5-benzylated 4-oxo-3,4-dihydro-5H-pyridazino[4,5-b]indoles as PI3Kα inhibitors, Eur. J. Med. Chem. 57 (2012) 225–233.
[15] G. Burgy, E. Limanton, F. Carreaux, E. Durieu, L. Meijer, J.-P. Bazureau, Exploring the Synthesis of New 1-(4-Substitutedphenylamino)imidazo[1,5-a]indol-3-one derivatives as cyclized analogs of leucettines, J. App. Pharm. Sci. 4 (2014) 025–032.
[16] K.F. Byth, J.D. Culshaw, S. Green, S.E. Oakes, A.P. Thomas, Imidazo[1,2-a]pyridines. Part 2: SAR and optimisation of a potent and selective class of cyclin-dependent kinase inhibitors, Bioorg. Med. Chem. Lett. 14 (2004) 2245–2248.
[17] R.P. Hertzberg, A.J. Pope, High-throughput screening: new technology for the 21st century, Curr. Opin. Chem. Biol. 4 (2000) 445–451.
[18] I. Ferrer, M. Barrachina, B. Puig, M. Martínez de Lagrán, E. Martí, J. Avila, M. Dierssen, Constitutive Dyrk1A is abnormally expressed in alzheimer disease, down syndrome, pick disease, and related transgenic models, Neurobiol. Dis. 20 (2005) 392–400.
[19] M. Mariano, R.W. Hartmann, M. Engel, Systematic diversification of benzylidene heterocycles yields novel inhibitor scaffolds selective for Dyrk1A, Clk1 and CK2, Eur. J. Med. Chem. 112 (2016) 209–216.
[20] W.-J. Song, L.R. Sternberg, C. Kasten-Sportès, M.L.V. Keuren, S.-H. Chung, A.C. Slack, D.E. Miller, T.W. Glover, P.-W. Chiang, L. Lou, D.M. Kurnit, Isolation of human and murine homologues of thedrosophilaminibrain gene: human homologue maps to 21q22.2 in the down syndrome “critical region”, Genomics 38 (1996) 331–339.
[21] Y. Ogawa, Y. Nonaka, T. Goto, E. Ohnishi, T. Hiramatsu, I. Kii, M. Yoshida, T. Ikura, H. Onogi, H. Shibuya, T. Hosoya, N. Ito, M. Hagiwara, Development of

a novel selective inhibitor of the Down syndrome-related kinase Dyrk1A, Nat. Commun. 1 (2010) 86.
[22] J. Princi, K. Chandrabose, N.S.H.N. Moorthy, W. Digambar Kumar, J. Arvind Kumar, T. Piyush, Human CDC2-Like Kinase 1 (CLK1): a novel target for Alzheimer's disease, Curr. Drug Targets 15 (2014) 539–550.
[23] Y. Sato, Y. Onozaki, T. Sugimoto, H. Kurihara, K. Kamijo, C. Kadowaki, T. Tsujino, A. Watanabe, S. Otsuki, M. Mitsuya, M. Iida, K. Haze, T. Machida, Y. Nakatsuru, H. Komatani, H. Kotani, Y. Iwasawa, Imidazopyridine derivatives as potent and selective Polo-like kinase (PLK) inhibitors, Bioorg. Med. Chem. Lett. 19 (2009) 4673–4678.
[24] K.S. Gudmundsson, S.D. Boggs, J.G. Catalano, A. Svolto, A. Spaltenstein, M. Thomson, P. Wheelan, S. Jenkinson, Imidazopyridine-5,6,7,8-tetrahydro-8-quinolinamine derivatives with potent activity against HIV-1, Bioorg. Med. Chem. Lett. 19 (2009) 6399–6403.
[25] W. An, W. Wang, T. Yu, Y. Zhang, Z. Miao, T. Meng, J. Shen, Discovery of novel 2-phenyl-imidazo[1,2-a]pyridine analogues targeting tubulin polymerization as antiproliferative agents, Eur. J. Med. Chem. 112 (2016) 367–372.
[26] A. Gueiffier, M. Lhassani, A. Elhakmaoui, R. Snoeck, G. Andrei, O. Chavignon, J.-C. Teulade, A. Kerbal, E.M. Essassi, J.-C. Debouzy, M. Witvrouw, Y. Blache, J. Balzarini, E. De Clercq, J.-P. Chapat, Synthesis of acyclo-c-nucleosides in the imidazo[1,2-a]pyridine and pyrimidine series as antiviral agents, J. Med. Chem. 39 (1996) 2856–2859.
[27] N. Dahan-Farkas, C. Langley, A.L. Rousseau, D.B. Yadav, H. Davids, C.B. de Koning, 6-Substituted imidazo[1,2-a]pyridines: synthesis and biological activity against colon cancer cell lines HT-29 and Caco-2, Eur. J. Med. Chem. 46 (2011) 4573–4583.
[28] W. Han, D.L. Menezes, Y. Xu, M.S. Knapp, R. Elling, M.T. Burger, Z.-J. Ni, A. Smith, J. Lan, T.E. Williams, J. Verhagen, K. Huh, H. Merritt, J. Chan, S. Kaufman, C.F. Voliva, S. Pecchi, Discovery of imidazo[1,2-a]-pyridine inhibitors of pan-PI3 kinases that are efficacious in a mouse xenograft model, Bioorg. Med. Chem. Lett. 26 (2016) 742–746.
[29] Y. Rival, G. Grassy, A. Taudou, R. Ecalle, Antifungal activity in vitro of some imidazo[1,2-a]pyrimidine derivatives, Eur. J. Med. Chem. 26 (1991) 13–18.
[30] K.C. Rupert, J.R. Henry, J.H. Dodd, S.A. Wadsworth, D.E. Cavender, G.C. Olini, B. Fahmy, J.J. Siekierka, Imidazopyrimidines, potent inhibitors of p38 MAP kinase, Bioorg. Med. Chem. Lett. 13 (2003) 347–350.
[31] Z.-P. Zhuang, M.-P. Kung, A. Wilson, C.-W. Lee, K. Plössl, C. Hou, D.M. Holtzman, H.F. Kung, Structure–activity relationship of imidazo[1,2-a] pyridines as ligands for detecting β-Amyloid plaques in the brain, J. Med. Chem. 46 (2003) 237–243.
[32] Y. Uto, Imidazo 1,2-a pyridines as cholesterol 24-hydroxylase (CYP46A1) inhibitors: a patent evaluation (WO2014061676), Expert Opin. Ther. Pat. 25 (2015) 373–377.
[33] N.P. Buu-Hoï, P. Jacquignon, N.D. Xuong, D. Lavit, 2-Arylpyrrocolines and 2-arylpyrimidazoles, J. Org. Chem. 19 (1954) 1370–1375.
[34] S.-Y. Takizawa, J.-I. Nishida, T. Tsuzuki, S. Tokito, Y. Yamashita, Synthesis and characterization of novel iridium complexes with ligands of 2-phenylimidazo [1,2-a]pyridine derivatives and application to organic light-emitting diode, Chem. Lett. 34 (2005) 1222–1223.
[35] J. Koubachi, S. El Kazzouli, S. Berteina-Raboin, A. Mouaddib, G. Guillaumet, Synthesis of polysubstituted imidazo[1,2-a]pyridines via microwave-assisted one-pot cyclization/suzuki coupling/palladium-catalyzed heteroarylation, J. Org. Chem. 72 (2007) 7650–7655.
[36] R. Frédérick, C. Bruyère, C. Vancraeynest, J. Reniers, C. Meinguet, L. Pochet, A. Backlund, B. Masereel, R. Kiss, J. Wouters, Novel trisubstituted harmine derivatives with original in vitro anticancer activity, J. Med. Chem. 55 (2012) 6489–6501.
[37] T. Tahtouh, J.M. Elkins, P. Filippakopoulos, M. Soundararajan, G. Burgy, E. Durieu, C. Cochet, R.S. Schmid, D.C. Lo, F. Delhommel, A.E. Oberholzer, L.H. Pearl, F. Carreaux, J.-P. Bazureau, S. Knapp, L. Meijer, Selectivity, cocrystal structures, and neuroprotective properties of leucettines, a family of protein kinase inhibitors derived from the marine sponge alkaloid leucettamine B, J. Med. Chem. 55 (2012) 9312–9330.
[38] G. Manning, D.B. Whyte, R. Martinez, T. Hunter, S. Sudarsanam, The protein kinase complement of the human genome, Science 298 (2002) 1912–1934.
[39] T. Yin, M.J. Lallena, E.L. Kreklau, K.R. Fales, S. Carballares, R. Torrres, G.N. Wishart, R.T. Ajamie, D.M. Cronier, P.W. Iversen, T.I. Meier, R.T. Foreman, D. Zeckner, S.E. Sissons, B.W. Halstead, A.B. Lin, G.P. Donoho, Y. Qian, S. Li, S. Wu, A. Aggarwal, X.S. Ye, J.J. Starling, R.B. Gaynor, A. de Dios, J. Du, A novel CDK9 inhibitor shows potent antitumor efficacy in preclinical hematologic tumor models, Mol. Cancer Ther. 13 (2014) 1442–1456.
[40] A.N. Bullock, S. Das, J.É. Debreczeni, P. Rellos, O. Fedorov, F.H. Niesen, K. Guo, E. Papagrigoriou, A.L. Amos, S. Cho, B.E. Turk, G. Ghosh, S. Knapp, Kinase domain insertions define distinct roles of CLK kinases in SR protein phosphorylation, Structure 17 (2009) 352–362.
[41] K. Anderson, Y. Chen, Z. Chen, R. Dominique, K. Glenn, Y. He, C. Janson, K.-C. Luk, C. Lukacs, A. Polonskaia, Q. Qiao, A. Railkar, P. Rossman, H. Sun, Q. Xiang, M. Vilenchik, P. Wovkulich, X. Zhang, Pyrido[2,3-d]pyrimidines: discovery and preliminary SAR of a novel series of DYRK1B and DYRK1A inhibitors, Bioorg. Med. Chem. Lett. 23 (2013) 6610–6615.
[42] O. Fedorov, K. Huber, A. Eisenreich, P. Filippakopoulos, O. King, A.N. Bullock, D. Szklarczyk, L.J. Jensen, D. Fabbro, J. Trappe, U. Rauch, F. Bracher, S. Knapp, Specific CLK inhibitors from a novel chemotype for regulation of alternative splicing, Chem. Biol., 18 67–76.
[43] C. Bissantz, B. Kuhn, M. Stahl, A medicinal chemist's guide to molecular interactions, J. Med. Chem. 53 (2010) 5061–5084.
[44] S.-L. Liu, C. Wang, T. Jiang, L. Tan, A. Xing, J.-T. Yu, The role of Cdk5 in Alzheimer's disease, Mol. Neurobiol. (2015) 1–15.
[45] S. Bach, M. Knockaert, J. Reinhardt, O. Lozach, S. Schmitt, B. Baratte, M. Koken, S.P. Coburn, L. Tang, T. Jiang, D.-c. Liang, H. Galons, J.-F. Dierick, L.A. Pinna, F. Meggio, F. Totzke, C. Schächtele, A.S. Lerman, A. Carnero, Y. Wan, N. Gray, L. Meijer, Roscovitine targets, protein kinases and pyridoxal kinase, J. Biol. Chem. 280 (2005) 31208–31219.
[46] H. Zegzouti, M. Zdanovskaia, K. Hsiao, S.A. Goueli, ADP-Glo: a bioluminescent and homogeneous ADP monitoring assay for kinases, Assay. Drug Dev. Technol. 7 (2009) 560–572.
[47] J. Sadowski, J. Gasteiger, G. Klebe, Comparison of automatic three-dimensional model builders using 639 X-ray structures, J. Chem. Inf. Comput. Sci. 34 (1994) 1000–1008.
[48] G. Jones, P. Willett, R.C. Glen, A.R. Leach, R. Taylor, Development and validation of a genetic algorithm for flexible docking1, J. Mol. Biol. 267 (1997) 727–748.
[49] O. Korb, T. Stützle, T.E. Exner, Empirical scoring functions for advanced protein–ligand docking with PLANTS, J. Chem. Inf. Model. 49 (2009) 84–96.
[50] E.F. Pettersen, T.D. Goddard, C.C. Huang, G.S. Couch, D.M. Greenblatt, E.C. Meng, T.E. Ferrin, UCSF Chimera—A visualization system for exploratory research and analysis, J. Comput. Chem. 25 (2004) 1605–1612.